Fabrication of Superhydrophobic SA-CeO$_2$@Cu Mesh and Its Application in Oil−Water Separation

Ting Liang,* Biao Wang, Zhenzhong Fan,* and Qingwang Liu

Read Online

ACCESS | Metrics & More | Article Recommendations

ABSTRACT: CeO$_2$ was synthesized by the co-precipitation method on the Cu mesh substrate and modified the surface of CeO$_2$@Cu mesh by stearic acid (SA). The superhydrophobic behavior was ascribed to the combination of hierarchical micro−nanostructure of CeO$_2$ and the hydrophobic alkyl groups from SA. The SA-CeO$_2$@Cu mesh had antiacid and base stability and excellent durability as well as high separation efficiency. The separation efficiency can be up to 98.0% after separating 30 times.
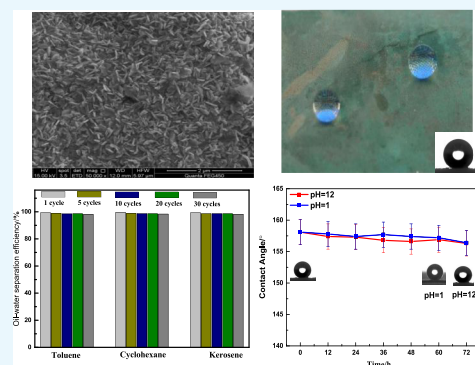
INTRODUCTION

It is pretty difficult to treat the increasing emissions of industrial oily wastewater because of the pressure of environmental protection and ecological balance. Therefore, the treatment of oily wastewater is one of the urgent problems in the field of environmental engineering. The traditional methods, such as flotation method,[1,2] flocculation method,[3] etc., have been unable to meet the current environmental requirements, and it is imperative to adopt new, efficient, and functional oil absorption or oil−water separation materials. Superhydrophobic and superhydrophilic materials[4−7] have received great attention due to their potential application in oil−water separation. Only oil can pass through these materials due to their superhydrophilicity, while water is totally repelled due to their superhydrophobicity. Superhydrophobic−superhydrophilic surface has unique advantages, such as self-cleaning effect,[8,9] superhydrophobic materials have properties of antifouling,[10,11] anticorrosion,[12,13] anti-icing,[14,15] drag reduction,[16,17] etc. Due to the large difference in surface tension between the oil phase and the water phase in the oil−water mixture, superhydrophobic materials can be used as the difference to selectively remove water or oil, thereby achieving efficient oil−water separation.

Many artificial superhydrophobic membrane materials, such as metallic meshes,[18,19] sponge,[20,21] and ceramic materials,[22,23] etc, have become the focus of research on oil−water separation materials due to their high flux, low cost, simple operation, and high processing efficiency.

As we know, proper roughness and low surface energy are the key factors to prepare superhydrophobic surfaces.[24−26] The proper roughness is useful to improve the performance of filtration membranes. The relationship between surface roughness and water repellency was worked out by Cassie and Baxter[27] as well as Wenzel.[28] Various methods are used to fabricate superhydrophobic surfaces, such as self-assembly,[29,30] electrospinning,[31] sol−gel methods,[32] etc. Many researchers have studied the practical applications of superhydrophobic materials. However, the poor stability and reusability of superhydrophobic materials seriously hindered their practical applications. It is urgently necessary to design superhydrophobic materials that have low cost and high separation efficiency and are environmentally friendly for oil−water separation. The membrane separation method is widely used in the treatment of oily wastewater because of its simple operation, good treatment effect, no secondary pollution, and low-energy consumption.

Recently, Azimi et al. reported that rare-earth oxide (REO) surfaces showed their thermally stable hydrophobicity after exposure to 1000 °C.[33] Moreover, Azimi et al. also revealed that REOs become superhydrophobic with textured morphology. Compared with organic metals, these inorganic REOs are thermally and mechanically more stable, which allows us to use them as a novel durable hydrophobic coating. Zenkin et al.[34]
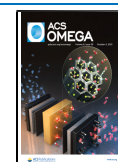
prepared Nd_2O_3, La_2O_3, and Y_2O_3 by the sputtering method and proved that the hydrophobicity was related to the nonpolar component of the surfaces of REOs. CeO_2 is an inexpensive and widely used rare-earth compound with N-type semiconductor properties and a unique 4f electronic structure. It exhibits excellent oxygen storage and charge exchange capacity and is widely used in three-way catalysts, photocatalysis, wastewater treatment, electronic ceramics, etc. As a surface modifier, SA has nontoxic biocompatibility, and it is not easy to change the physical and chemical properties of the powder. The surfaces of metallic meshes have been modified by low-energy materials or nanoparticles to form superhydrophobic and superoleophilic for oil−water separation. According to the different mesh shapes and densities, the function of the copper mesh is different. The main role of copper mesh is screening, filtration, protection, etc. However, as far as we know, no works have reported the SA-CeO_2@Cu mesh with superhydrophobic and superoleophilic properties for oil−water separation.

Herein, we report a superhydrophobic and superoleophilic CeO_2-coated Cu mesh by the co-precipitation method and calcination and then used SA as a low-energy material. In addition, the SA-CeO_2@Cu mesh showed desirable stability and high oil−water separation efficiency when suffered from acid and base. The prepared SA-CeO_2@Cu mesh was also characterized. The oil−water separation experiments and the recyclability of SA-CeO_2@Cu mesh were also investigated.

■ RESULTS AND DISCUSSION

X-ray Diffraction (XRD) Analysis. As shown in Figure 1a,b, the XRD pattern of CeO_2 and SA-CeO_2 were consistent
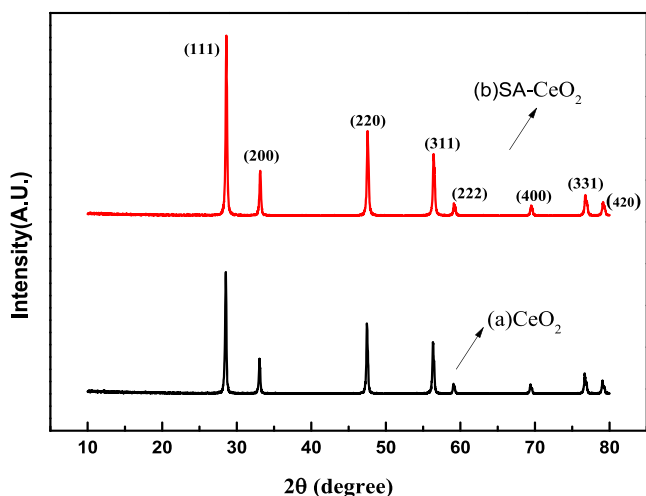

Figure 1. Image of XRD pattern of (a) CeO_2 and (b) SA-CeO_2.

with the values in the standard card (JCPDS No. 34-0394). The diffraction peaks observed at 2θ values of 27.28, 33.58, 46.46, 57.08, 59.26, 68.88, 76.48, and 78.82° can be assigned to the (111), (200), (220), (311), (222), (400), (331), and (420) crystal planes of fluorite, respectively. The XRD pattern of SA-CeO_2 was similar to that of CeO_2 without any peaks attributed to the SA molecules, indicating that the crystalline phase of CeO_2 did not change after the treatment with SA.

FT-IR Analysis. As shown in Figure 2a, the broad peak around 3400 cm^{-1} was the bond stretching vibration absorption peak and the characteristic peak of the crystal
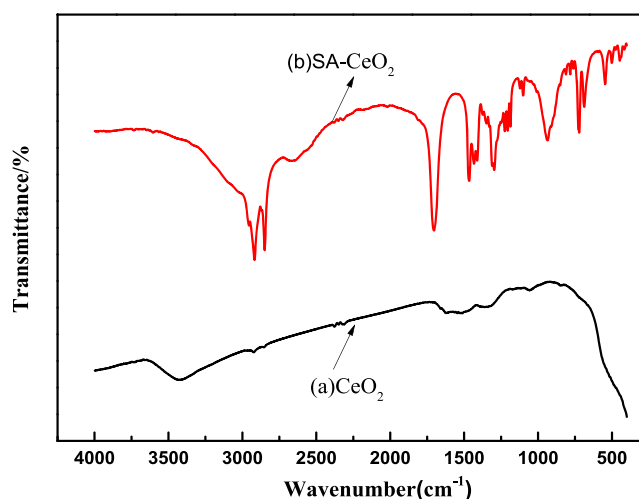

Figure 2. FT-IR spectrum of (a) CeO_2 and (b) SA-CeO_2.

water, which indicated that the sample contains crystal water. The surface modification process of CeO_2 was a process in which the carboxyl group in SA reacted with the hydroxyl group on the surface of CeO_2 to change the surface properties of CeO_2. Compared with the unmodified CeO_2, the broad peak of SA-CeO_2 around 3400 cm^{-1} was the disappearance of the −OH stretching vibration absorption peak, indicating that the carboxyl group in SA was chemically bonded to the hydroxyl group on the surface of CeO_2. As shown in Figure 2b, the characteristic absorption peak at 2924 and 2858 cm^{-1} were the −C−H stretching vibration peaks in −CH_2 and −CH_3. The carboxyl stretching vibration peak appeared at 1710 cm^{-1}, which was consistent with the fatty long carbon chain group in SA, which indicated the presence of SA on the surface of the modified CeO_2.

Morphological Analysis of the CeO_2@Cu Mesh. As shown in Figure 3, the microscopic morphology analysis of the surface of the untreated Cu mesh and the surface of the CeO_2@Cu mesh. As shown in Figure 3a, the surface looked smooth at low magnification. After calcination, a uniform rod-shaped CeO_2 with a size of about 100 nm was immobilized on the surface of CeO_2@Cu mesh, which provided a nanolevel roughness to the surface of the Cu mesh. Also, the CeO_2 nanoparticles exhibit immobilization with a resistance sonication in ethanol for 30 min with a significant amount of CeO_2 nanoparticles still anchored on the Cu mesh surface. The CeO_2@Cu mesh had a micro−nano-level layered structure, in which CeO_2 nanoparticles were fixed on the surface of the copper mesh wire, which was the key factor for superhydrophobicity.[35] The CeO_2 nanoparticles can effectively reduce the contact area between the water drops and Cu mesh.

Wettability Tests and Adhesion Performance Analysis. As shown in Figure 4a, the CA of water droplets on the untreated copper mesh was 82.1 ± 2°, and the oil droplets would spread out quickly on the untreated copper mesh. As shown in Figure 4b−d, the CA of water droplets on the CeO_2@Cu mesh was 137.5 ± 2°, and the CAs of the SA-CeO_2@Cu mesh immersed in SA for 1 h and 12 h were 150.1 ± 2° and 158.1 ± 2°, respectively. Due to the capillary effect produced by the microstructure, water was prevented from passing through the SA-CeO_2@Cu mesh. The micro-/nanostructure can reduce the contact area between the solid−liquid and water and low surface energy SA, which
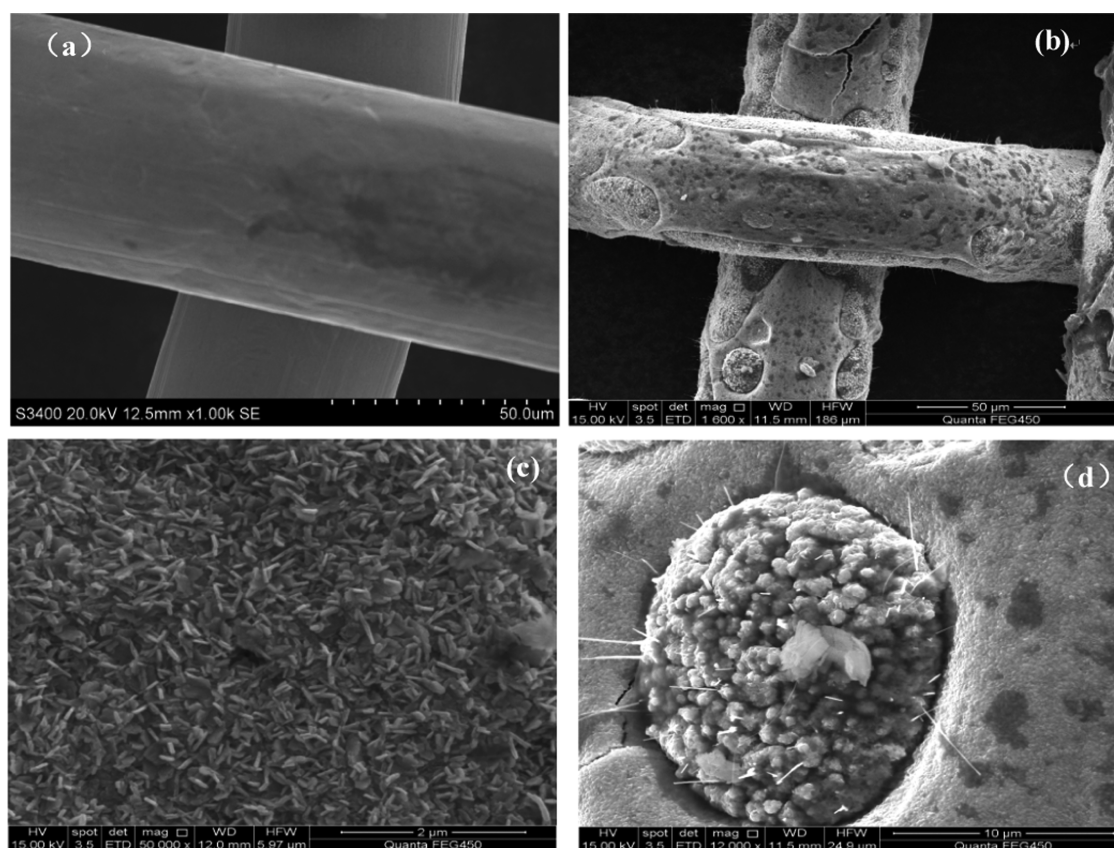
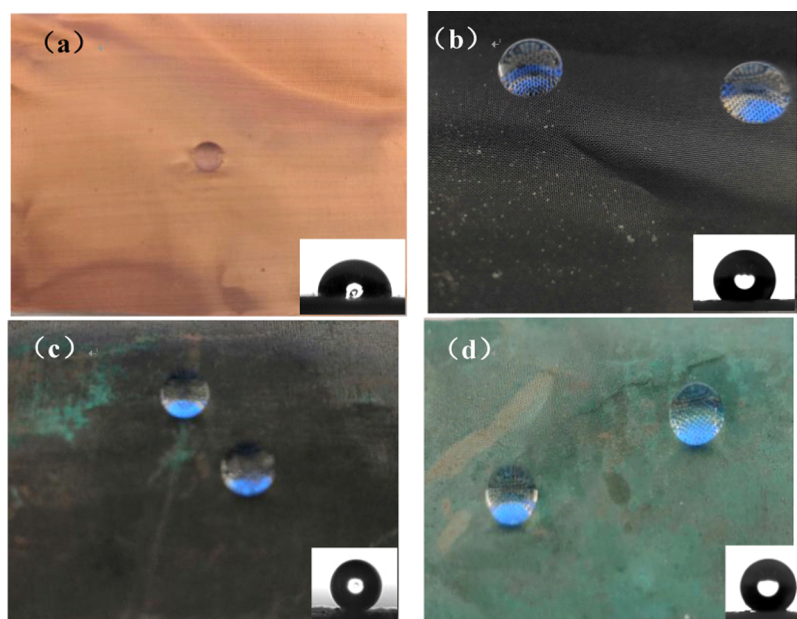**Figure 3.** SEM images of (a) the untreated Cu mesh and (b)−(d) CeO$_2$@Cu mesh.

Figure 4. CA on different Cu mesh surfaces water droplets on (a) untreated Cu mesh, (b) CeO$_2$@Cu mesh, (c) CeO$_2$@Cu mesh for 1 h, and (d) CeO$_2$@Cu mesh for 12 h.

reacted with the Cu mesh to generate copper stearate. The SA-CeO$_2$@Cu mesh showed low adhesion to water.

To have a better understanding of the superhydrophobic behavior of the SA-CeO$_2$@Cu mesh, the wetting state and the oil−water separation performance were studied. Due to the modification of the low-energy material SA together with CeO$_2$ nanoparticles, water droplets would be in the superhydropho-bic Cassie state and high WCA can be explained by the Cassie−Baxter equation[27,36] as follows.

$$\cos\ \theta_2 = f_1 \cos\ \theta_1 - f_2 \tag{1}$$

where θ_2 is the WCA on the SA-CeO$_2$@Cu mesh, θ_1 is the WCA on the original Cu mesh, and f_1 and f_2 ($f_1 + f_2 = 1$) are the area frictions of water connecting with the SA-CeO$_2$@Cu

Figure 5. Adhesion images of the water droplets on the SA-CeO$_2$@Cu mesh.

mesh and air, respectively. According to eq 2, f_2 can be calculated to be 0.937, indicating that 93.7% surface area was covered by air, which resulted in the superhydrophobicity of the SA-CeO$_2$@Cu mesh. According to the Wenzel equation,[28] the superoleophilic properties can be enhanced by the nanostructures. Therefore, when placed on the SA-CeO$_2$@ Cu mesh, the oil droplet would enter the nanostructures due to the capillary effect. The combination of the hydrophobic surface chemistry and roughness would lead to super-hydrophobic and superoleophilic properties easily.

As shown in the low adhesion image of water droplets and the SA-CeO$_2$@Cu mesh in Figure 5, 5 μL water droplets were suspended on the needle tube. By controlling the experimental platform, the water droplets contacted with the surface of the SA-CeO$_2$@Cu mesh. Continuous rise in the experimental platform caused the water droplets and the surface of the SA-CeO$_2$@Cu mesh to squeeze; then, as the experimental platform descended, the water droplets and the surface of the SA-CeO$_2$@Cu mesh completely separated.

When the SA-CeO$_2$@Cu mesh and the water droplets were completely separated, the water droplets recovered their original appearance and were fully suspended on the needle tube, and no liquid was adhered to the surface of the SA-CeO$_2$@Cu mesh, indicating that the prepared SA-CeO$_2$@Cu mesh surface had low adhesion to water droplets, and low adhesion performance was very important for superhydrophobic surfaces in the practical application of self-cleaning.

Oil–Water Separation. Toluene, cyclohexane, and kerosene were chosen as the oil phases. The separation efficiency of different oil–water mixtures when the mass of the oil phase was 10.0 g and the oil–water mass ratio was 1:1 is shown in Figure 6.

The separation efficiency of SA-CeO$_2$@Cu mesh was calculated by eq 2. For the oil–water mixture with a mass ratio of 1:1, the first separation efficiency was as high as 99%.
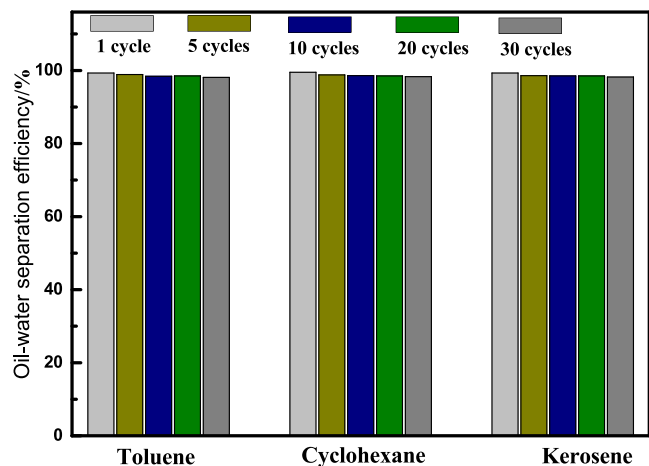
After several separation cycles, the separation efficiency can reach more than 98%, indicating that the SA-CeO$_2$@Cu mesh still maintained the water–oil separation ability. In addition, the SA-CeO$_2$@Cu mesh can separate different oil–water mixtures (water–cyclohexane, water–toluene, water–kerosene), indicating that the SA-CeO$_2$@Cu mesh can generally separate oil–water mixture. After 30 separation cycles, the oil–water separation efficiency of the SA-CeO$_2$@Cu mesh is still above 98%, indicating that it can be used as a filmlike material to efficiently separate an oil–water mixture, and the mechanical stability of the Cu mesh was excellent.

Chemical Stability. Chemical stability is important for practical applications. Therefore, to examine its chemical stability, the SA-CeO$_2$@Cu mesh was immersed into an acid solution (HCl, pH = 1) and a base solution (NaOH, pH = 12) for 72 h; then, the wettabilities and oil–water separation experiment of the SA-CeO$_2$@Cu mesh were investigated.

As shown in Figure 7, after immersing for 72 h, the CA in the hydrochloric acid solution with pH 1 was 156.3 ± 2° and that in the sodium hydroxide solution with pH 12 was 156.4 ± 2°; the oil–water separation efficiency remained above 98%, indicating that the SA-CeO$_2$@Cu mesh still maintained superhydrophobicity, which proved the excellent acid and alkali resistance of the SA-CeO$_2$@Cu mesh.

CONCLUSIONS

To summarize, the superhydrophobic and superoleophilic SA-CeO$_2$@Cu mesh was prepared with the Cu mesh as the substrate and SA as the substance with low surface energy. The SA-CeO$_2$@Cu mesh had chemical stability (e.g., immersed in acid, base) and excellent durability. The SA-CeO$_2$@Cu mesh can separate different oils that are insoluble in water and had a separation efficiency above 98% after 30 separation cycles. The excellent reusability and the high separation efficiency result in the possibility of the practical application of the SA-CeO$_2$@Cu mesh for oil–water separation.

EXPERIMENTAL SECTION

Materials. Cerium nitrate hexahydrate (Ce(NO$_3$)$_3$·6H$_2$O), oxalic acid (H$_2$C$_2$O$_4$), and SA were purchased from Aladdin (Shanghai China). Distilled water was made in our laboratory. Kerosene, cyclohexane, and toluene were purchased from Aladdin (Shanghai China). All reagents were analytical grade and used without further purification or modification. Cu mesh (copper content >99%, 3 cm × 3 cm) with a pore size of about 75 μm was obtained from Jiangxi Dali Mesh Co., Ltd., China.

Fabrication of Superhydrophobic Surfaces. The Cu mesh was rinsed with ethanol and deionized water respectively and then dried at 80 °C for 30 min. The cleaned Cu mesh was immersed into a mixed solution containing cerium nitrate and oxalic acid. The concentration of cerium nitrate and oxalic acid was 0.1 and 0.2 mol/L, respectively. The Cu mesh with the mixed solution was stirred at the speed of 1000 rpm for 1 h.
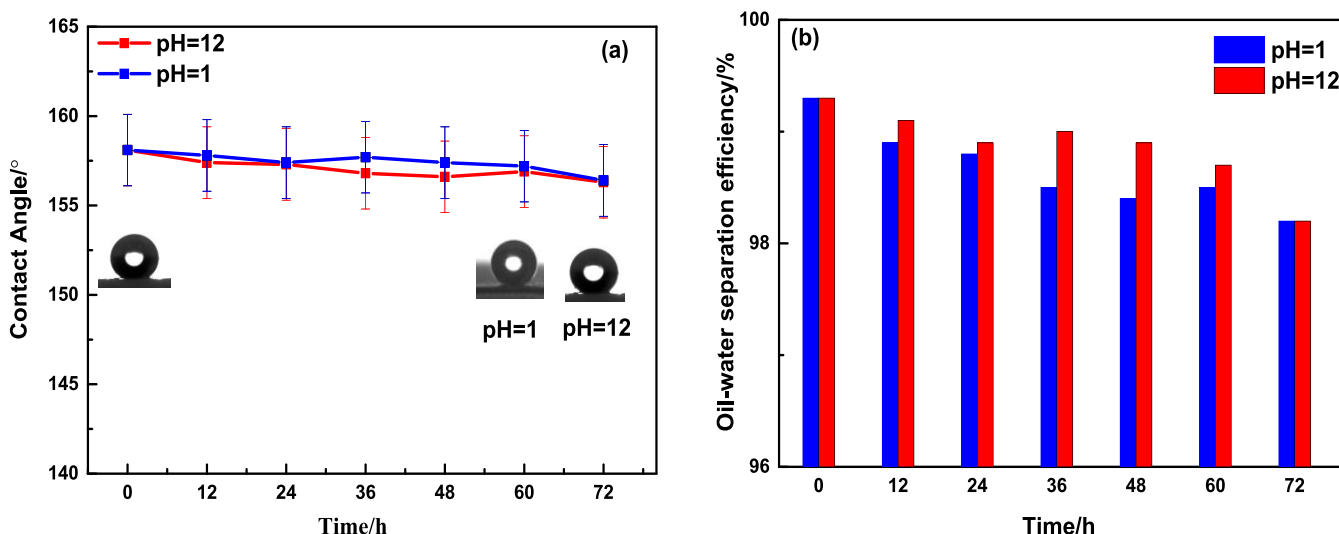

Figure 6. Separation efficiency with different separation times.

Figure 7. (a) CA at different immersion times. (b) Separation efficiency at different immersion times.

Then, the CeO$_2$@Cu mesh was calcined at a programmable muffle furnace at 450 °C for 4 h under a nitrogen atmosphere.

The coated Cu mesh was immersed in 1 wt % SA, which was dispersed in absolute ethanol for 1 h at 25 °C. Finally, the CeO$_2$@Cu mesh modified with SA (SA-CeO$_2$@Cu mesh) was washed thoroughly with absolute ethanol and then dried at 80 °C for 30 min in a vacuum drying oven.

Oil−Water Separation Experiment. In this experiment, the oil−water separation experiment can be carried out only by the gravity drive of the oil and water phase. After taking a large beaker and a small beaker, the prepared SA-CeO$_2$@Cu mesh was put above the small beaker and the different proportions of kerosene, cyclohexane, and toluene with water were measured. The oil−water mixture was stirred with a glass rod before oil−water separation. During the continuous stirring process, the oil−water mixture is directly poured from the top of the separation device to observe the separation effect of the water−oil mixture. The oil−water separation device is shown in Figure 8.
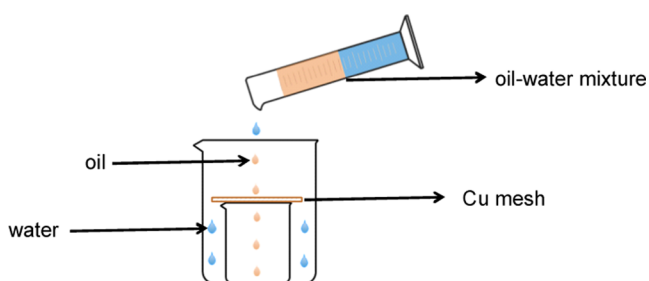

Figure 8. Schematic diagram of the oil−water separation device.

The oil−water separation efficiency was calculated by eq 2

$$\eta = m_1/m \times 100\% \tag{2}$$

where m_1 is the oil after oil−water separation, m is the volume of the initial oil, and η is the separation efficiency.

Characterization. X-ray diffraction (XRD) patterns of the samples were recorded using a Bruker D8 with Cu Kα radiation. The crystalline size of CeO$_2$ and was calculated from the Scherrer equation. The micro- and nanoscale morphologies of the SA-CeO$_2$@Cu mesh were analyzed by field emission scanning electron microscopy (FESEM, QUANTA FEG450). Water contact angle (WCA) measurements were carried out to investigate the superhydrophobicity and superoleophilicity of the CeO$_2$@Cu mesh with a JY-PHB using a droplet (5 μL) of distilled water. All of the WCAs were measured at five different spots on each sample surface and then the average value was taken. The Fourier transform infrared spectroscopy (FT-IR) was performed using Thermo Nicolet with the scanning wavenumber range of 4500−400 cm^{-1}.

■ AUTHOR INFORMATION

Corresponding Authors

Ting Liang − *South China Advanced Institute for Soft Matter Science and Technology, South China University of Technology, Guangzhou 510006, P. R. China; Guangdong Provincial Key Laboratory of Functional and Intelligent Hybrid Materials and Devices, South China University of Technology, Guangzhou 510640, P. R. China; School of Petroleum Engineering, Northeast Petroleum University, Daqing 163000, P. R. China;* ⊙ orcid.org/0000-0003-3783-4191; Email: lt900201@scut.edu.cn

Zhenzhong Fan − *School of Petroleum Engineering, Northeast Petroleum University, Daqing 163000, P. R. China;* Email: fanzhenzhong@nepu.edu.cn

Authors

Biao Wang − *School of Petroleum Engineering, Northeast Petroleum University, Daqing 163000, P. R. China*

Qingwang Liu − *School of Petroleum Engineering, Northeast Petroleum University, Daqing 163000, P. R. China*

Complete contact information is available at:
https://pubs.acs.org/10.1021/acsomega.1c03128

Author Contributions

T.L. and B.W. contributed equally to the work and are co-first authors. T.L. and Z.F. initiated the project. T.L. and B.W. were supervised by Z.F. and Q.L. T.L. prepared the superhydrophobic surfaces. B.W. performed the oil−water separation experiment.

Notes

The authors declare no competing financial interest.

REFERENCES

(1) Hami, M. L.; Alhashimi, M. A.; Aldoori, M. M. Effect of Activated Carbon on BOD and COD Removal in a Dissolved Air Flotation Unit Treating Refinery Wastewater. *Desalination* **2007**, *216*, 116−122.

(2) Xu, H.; Liu, J.; Wang, Y.; et al. Oil Removing Efficiency in Oil-Water Separation Flotation Column. *Desalin. Water Treat.* **2015**, *53*, 2456−2463.

(3) Huang, B.; Xiaohui, L.; et al. Study on Demulsification-Flocculation Mechanism of Oil-Water Emulsion in Produced Water from Alkali/Surfactant/Polymer Flooding. *Polymers* **2019**, *11*, No. 395.

(4) Li, F.; Bhushan, B.; Pan, Y.; et al. Bioinspired Superoleophobic/superhydrophilic Functionalized Cotton for Efficient Separation of Immiscible Oil-Water Mixtures and Oil-Water Emulsions. *J. Colloid Interface Sci.* **2019**, *548*, 123−130.

(5) Khosravi, M.; Azizian, S. Preparation of Superhydrophobic and Superoleophilic Nanostructured Llayer on Steel Mesh for Oil-water Separation. *Sep. Purif. Technol.* **2017**, *172*, 366−373.

(6) Qing, W.; Shi, X.; Deng, Y.; et al. Robust Superhydrophobic-superoleophilic Polytetrafluoroethylene Nanofibrous Membrane for Oil/water Separation. *J. Membr. Sci.* **2017**, *540*, 354−361.

(7) Lim, Y. T.; Han, N.; Jang, W.; et al. Surface Design of Separators for Oil/water Separation with High Separation Capacity and Mechanical Stability. *Langmuir* **2017**, *33*, 8012−8022.

(8) Kumar, A.; Gogoi, B. Development of Durable Self-cleaning Superhydrophobic Coatings for Aluminium Surfaces via Chemical Etching Method. *Tribol. Int.* **2018**, *122*, 114−118.

(9) Sasmal, A. K.; Mondal, C.; Sinha, A. K.; et al. Fabrication of Superhydrophobic Copper Surface on Various Substrates for Roll-off, Self-Cleaning, and Water/Oil Separation. *ACS Appl. Mater. Interfaces* **2014**, *6*, 22034−22043.

(10) Gao, S. W.; Huang, J. Y.; Li, S. H.; et al. Facile Construction of Robust Fluorine-free Superhydrophobic $TiO_2@$fabrics with Excellent Anti-fouling, Water-oil Separation and UV-protective Properties. *Mater. Des.* **2017**, *128*, 1−8.

(11) Cao, C.; Ge, M.; Huang, J.; et al. Robust Fluorine-free Superhydrophobic PDMS-ormosil@fabrics for Highly Effective Self-cleaning and Efficient Oil-water Separation. *J. Mater. Chem. A* **2016**, *4*, 12179−12187.

(12) Chang, K. C.; Lu, H. I.; Peng, C. W.; et al. Nanocasting Technique to Prepare Lotus-leaf-like Superhydrophobic Electroactive Polyimide as Advanced Anticorrosive Coatings. *ACS Appl. Mater. Interfaces* **2013**, *5*, 1460−1467.

(13) Xu, H.; Liu, J.; Chen, Y.; et al. Facile Fabrication of Superhydrophobic Polyaniline Structures and their Anticorrosive Properties. *J. Appl. Polym. Sci.* **2016**, *133*, No. 44248.

(14) Farhadi, S.; Farzaneh, M.; Kulinich, S. A. Anti-icing Performance of Superhydrophobic Surfaces. *Appl. Surf. Sci.* **2011**, *257*, 6264−6269.

(15) Ruan, M.; Li, W.; Wang, B.; et al. Preparation and Anti-icing Behavior of Superhydrophobic Surfaces on Aaluminum Alloy Substrates. *Langmuir* **2013**, *29*, 8482−8491.

(16) McHale, G.; Newton, M. I.; Shirtcliffe, N. J. Immersed Superhydrophobic Surfaces: Gas Exchange, Slip and Drag Reduction Properties. *Soft Matter* **2010**, *6*, 714−719.

(17) Zhou, Y.; Li, M.; Su, B.; et al. Superhydrophobic Surface Created by the Silver Mirror Reaction and its Drag-reduction Effect on Water. *J. Mater. Chem.* **2009**, *19*, 3301−3306.

(18) Zhang, L.; Deng, X.; Hu, H.; et al. Superhydrophilic Al_2O_3 Composite Meshes for Continuous High-Efficiency Oil-Water Separation. *Mater. Lett.* **2020**, *274*, No. 127892.

(19) Khosravi, M.; Azizian, S.; Boukherroub, R. Efficient Oil/Water Separation by Superhydrophobic CuxS Coated on Copper Mesh. *Sep. Purif. Technol.* **2019**, *215*, 573−581.

(20) Lee, Y. S.; Lim.; et al. One-Step Synthesis of Environmentally Friendly Superhydrophilic and Superhydrophobic Sponges for Oil/Water Separation. *Materials* **2019**, *12*, No. 1182.

(21) Wang, F.; Lei, S.; Li, C.; et al. Superhydrophobic Cu Mesh Combined with a Superoleophilic Polyurethane Sponge for Oil Spill Adsorption and Collection. *Ind. Eng. Chem. Res.* **2014**, *53*, 7141−7148.

(22) Zhong, Z.; Xing, W.; Zhang, B. Fabrication of Ceramic Membranes with Controllable Surface roughness and Their Applications in Oil/water Separation. *Ceram. Int.* **2013**, *39*, 4355−4361.

(23) Su, C.; Xu, Y.; Wei, Z.; et al. Porous Ceramic Membrane with Superhydrophobic and Superoleophilic Surface for Reclaiming Oil from Oily Water. *Appl. Surf. Sci.* **2012**, *258*, 2319−2323.

(24) Zhang, Y.; Chen, Y.; Shi, L.; et al. Recent Progress of Double-structural and Functional Materials with Special Wettability. *J. Mater. Chem.* **2012**, *22*, 799−815.

(25) Liu, M.; Wang, S.; Jiang, L. Bioinspired Multiscale Surfaces with Special Wettability. *MRS Bull.* **2013**, *38*, 375−382.

(26) Liu, K.; Cao, M.; Fujishima, A.; et al. Bio-inspired Titanium Dioxide Materials with Special Wettability and their Applications. *Chem. Rev.* **2014**, *114*, 10044−10094.

(27) Cassie, A. B. D.; Baxter, S. Wettability of Porous Surfaces. *Trans. Faraday Soc.* **1944**, *40*, 546−551.

(28) Wenzel, R. N. Surface Roughness and Contact Angle. *J. Phys. Chem. A* **1949**, *53*, 1466−1467.

(29) Rahmawan, Y.; Xu, L.; Yang, S. Self-assembly of Nanostructures towards Transparent, Superhydrophobic Surfaces. *J. Mater. Chem. A* **2013**, *1*, 2955−2969.

(30) Gao, A.; Wu, Q.; Wang, D.; et al. A Superhydrophobic Surface Templated by Protein Self-Assembly and Emerging Application toward Protein Crystallization. *Adv. Mater.* **2016**, *28*, 579−587.

(31) Sarkar, M. K.; Ba, L. K.; He, F.; et al. Design of an Outstanding Super-hydrophobic Surface by Electro-spinning. *Appl. Surf. Sci.* **2011**, *257*, 7003−7009.

(32) Zhang, T. T.; Huang, J.; Zhang, R. Z.; et al. Highly Transparent Superhydrophobic Surfaces from Silica Aerogel by Sol-Gel Method. *Adv. Mater. Res.* **2013**, *756−759*, 150−153.

(33) Azimi, G.; Dhiman, R.; Kwon, H. M.; et al. Hydrophobicity of Rare-earth Oxide Ceramics. *Nat. Mater.* **2013**, *12*, 315−320.

(34) Zenkin, S.; Kos, Š.; Musil, J. Hydrophobicity of Thin Films of Compounds of Low-electronegativity Metals. *J. Am. Ceram. Soc.* **2014**, *97*, 2713−2717.

(35) Su, Y.; Ji, B.; Zhang, K.; et al. Nano to Micro Structural Hierarchy Is Crucial for Stable Superhydrophobic and Water-Repellent Surfaces. *Langmuir* **2010**, *26*, 4984−4989.

(36) Arbatan, T.; Fang, X.; Wei, S. Superhydrophobic and Oleophilic Calcium Carbonate Powder as a Selective Oil Sorbent with Potential Use in Oil Spill Clean-ups. *Chem. Eng. J.* **2011**, *166*, 787−791.